

## MULTI-MODEL ADAPTIVE REGULATION FOR AIRCRAFT DYNAMICS WITH DIFFERENT ZERO STRUCTURES

**Eric D. Peterson,**

Department of Mechanical Engineering & Mechanics  
Drexel University  
Philadelphia, Pennsylvania, 19104  
Email: edp24@drexel.edu

**Harry G. Kwatny\***

Department of Mechanical Engineering & Mechanics  
Drexel University  
Philadelphia, Pennsylvania, 19104  
Email: hkwatny@coe.drexel.edu

### ABSTRACT

*An adaptive regulator is designed for parameter dependent families of systems subject to changes in the zero structure. Since continuous adaptive regulation is limited by relative degree and right half plane zeros, a multiple model adaptive regulator is implemented. The two multiple model design subproblems, covering and switching, are addressed with LQR state feedback and Lyapunov function switch logic respectively. These two subproblems are combined into a set of Linear Matrix Inequalities (LMI) and concurrently solved. The multiple model design method is applied to longitudinal aircraft dynamics.*

### 1 Introduction

The importance of open loop zero structure for closed loop regulation has long been known, c.f. [1–3]. Moreover, continuous adaptive regulation methods [4] often omit systems with zero structure change. Multiple model adaptive control has been proposed to accommodate systems with diverse structure [5–7]. A multiple model adaptive controller selects a controller from a predefined set when the appropriate plant is unknown. In general, the set of controllers is finite although the family of plants may be continuous.

A parameter dependent family of plants may contain several subfamilies each with a distinct zero structure. A robust linear regulator design must be cognizant of the zero structure [2]. In fact, given two subfamilies with distinct zero structure, a regulator designed for plants from one subfamily will generically fail to

regulate plants in the other subfamily [8]. This bound on *simultaneous regulation* of subfamilies motivates the multiple model adaptive control design technique presented here.

The design of multiple model adaptive systems presents two subproblems: controller covering and switching. Controller covering ensures a stabilizing controller exists in the set of controllers for all possible contingencies. The switching subproblem is to select a stabilizing controller from the set of controllers. In general, controller covering is treated separately from switching and only a trial and error approach is available [5, 9]. A unified, algorithmic approach to controller covering and switching is presented in [10]. Both Linear Quadratic Regulator (LQR) design and quadratic Lyapunov stability may be cast as convex LMIs. If LQR design and quadratic Lyapunov stability are employed for the controller covering and switching subproblems respectively, then a single, unified LMI solves both subproblems. This unified approach is suitable for multi-model design automation.

The regulator design method developed in [10] is applied to a multi-input/multi-output, four state, longitudinal aircraft dynamics model with unknown center of gravity location. The (Taylor) linearized family of plants from the equilibrium surface have two distinct zero structures and thus form two plant subfamilies. A controller is designed for each subfamily.

This paper is organized as follows. Section 2 introduces linear regulation of parameter dependent plants, details the plant family construction, and relates zero dynamic structure to simultaneous regulation. Section 3 introduces the multiple model adaptive regulation (MMAR) subproblems. Section 4 obtains the MMAR design equations. Section 5 investigates the aircraft dy-

---

\*Address all correspondence to this author.

namics example and Section 6 summarizes the main conclusions.

## 2 Problem Statement

A family of plants with diverse zero structure is constructed and obstacles to simultaneous linear regulation are presented.

### 2.1 Parameter Dependent Systems

Consider feedback regulation of the parameter dependent, nonlinear system

$$\begin{aligned}\dot{x} &= f(x, u, \vartheta) \\ e &= h(x, \vartheta)\end{aligned}\quad (1)$$

where  $x \in R^n$ ,  $u \in R^m$  and  $e \in R^p$  is the regulated output error. The vector of unknown but bounded parameters  $\vartheta \in R^k$  may act as state disturbances or reference inputs and belong to a known class of signals governed by the linear system

$$\dot{\vartheta} = Z\vartheta \quad (2)$$

This paper considers only constant disturbances and set-points such that  $Z = 0_k$ . The family of plants, and hence the subfamilies of plants with equivalent zero structure, vary with  $\vartheta$ .

Regulation suggests a stable equilibrium such that  $e \rightarrow 0$  as  $t \rightarrow \infty$ . The equilibrium surface  $\mathcal{E}^*$  is the set of points  $(x, u, \vartheta)$  invariant under dynamics Eqn. (1) for which regulation succeeds,

$$\mathcal{E}^* = \{(x, u, \vartheta) | \mathcal{E}(x, u, \vartheta) = 0\} \quad (3)$$

The function  $\mathcal{E} : R^{n+m+k} \rightarrow R^{n+p}$  is defined as

$$\mathcal{E}(x, u, \vartheta) \equiv \begin{bmatrix} f(x, u, \vartheta) \\ h(x, \vartheta) \end{bmatrix}.$$

A family of parameter dependent, linear plants  $\mathcal{P}$  is obtained by Taylor linearization of system Eqn. (1) on the equilibrium surface  $\mathcal{E}^*$ .

**Definition 2.1.** *Each plant in the family of plants,  $p(\vartheta) \in \mathcal{P}$ , is the regulator problem*

$$\begin{aligned}\dot{x} &= A(\vartheta)x + B(\vartheta)u + E(\vartheta)\vartheta \\ \dot{\vartheta} &= Z\vartheta \\ e &= C(\vartheta)x + F(\vartheta)\vartheta\end{aligned}\quad (4)$$

whose construction is detailed below.

Plant matrices  $A$ ,  $B$ ,  $C$ ,  $E$ , and  $F$  are the partial derivatives evaluated at an equilibrium point  $(x^*, u^*, \vartheta^*)$ , e.g.

$$A = \frac{\partial}{\partial x} f(x, u, \vartheta)|_{x^*, u^*, \vartheta^*}, \text{ etc.}$$

The equilibrium surface is an implicit manifold of dimension  $k$  since Eqn. (3) is  $n + m + k$  variables with  $n + p$  constraint equations (per Section 2.2,  $m = p$  for square systems). Hence the set  $\{A(\vartheta), B(\vartheta), C(\vartheta), E(\vartheta), F(\vartheta)\}$  are uniquely defined by  $k$  parameters. Parameterization of the equilibrium manifold is detailed in Section 4.3.

Robust regulation with continuous state feedback control  $u = K(x, \vartheta)$  is considered in this paper. Hence,  $\{A(\vartheta), B(\vartheta), C(\vartheta)\}$  must be smooth in the parameter  $\vartheta$ . Moreover, the system matrix  $\Gamma$  must be full rank such that (3) can be solved for any  $\{E, F\}$  in an open neighborhood of  $\mathcal{E}^*$  as detailed in Section 2.2 below.

The parameter dependent linearized system may be written

$$\begin{aligned}\delta\dot{x} &= A(\vartheta)\delta x + B(\vartheta)\delta u + E(\vartheta)\delta\vartheta \\ \delta e &= C(\vartheta)\delta x + F(\vartheta)\delta\vartheta\end{aligned}\quad (5)$$

Then obtain each  $p(\vartheta)$  in Eqn. (4) by joining the disturbance model Eqn. (2) to Eqn. (5).

In the fortuitous case that Eqn. (1) is a linear system with linear parametric uncertainty, i.e. the  $A(\vartheta)$ , etc. are linear in  $\vartheta$ , the plant family is convex in  $\vartheta$ . The case of linear systems is solved in [10].

For general nonlinear systems Eqn. (1) the exogenous disturbances and parametric uncertainty are lumped together since the plant dynamics are not invariant to state translation. Moreover, the parameters  $\vartheta$  may fail to uniquely define the manifold  $\mathcal{E}^*$ . Computing a global parametric representation of an implicit manifold is difficult in general. The zero structure deficiencies described in Sec. 2.2 below further complicate these computations. Two local representations of the manifold  $\mathcal{E}^*$  are examined in Sec. 5.3.

### 2.2 Simultaneous Regulation

While the importance of system invertability [1] and zero structure [2] in regulation are well known, the loss of simultaneous regulation due to zero structure change is less well known.

Consider a parameter independent linear system with disturbance state vector  $\vartheta$

$$\begin{aligned}\dot{x} &= Ax + Bu + E\vartheta \\ \dot{\vartheta} &= Z\vartheta \\ e &= Cx + F\vartheta\end{aligned}\quad (6)$$

**Definition 2.2.** *Regulation requires both  $\lim_{t \rightarrow \infty} e(t) = 0$  and internal stability. Regulation in the presence of variation in the plant*

matrices  $A, B, C$  is known as robust regulation or structurally stable regulation.

Structurally stable regulation uses error feedback and incorporates an internal model of the external signals to be tracked and disturbances to be rejected.

**Definition 2.3.** [11] *The structurally stable linear regulator incorporates an internal model of  $Z$ .*

A matrix  $M$  incorporates an internal model of  $Z$  if the minimal polynomial of  $Z$  divides at least  $p$  invariant factors of  $M$ . The invariant factors of  $M$ , related to elementary divisors, motivate the Smith canonical form. The minimal matrix polynomial  $\mathcal{M}(Z)$  is the monic polynomial in  $Z$  of smallest degree  $d$  such that

$$\mathcal{M}(Z) = \sum_{i=0}^d c_i Z^i = 0$$

For the case  $Z = 0_k$ , the minimal polynomial has degree one regardless of  $k$ . Hence, if  $k > 0$ , an internal model of dimension equal to or greater than the number of outputs ( $p$ ) is sufficient for robust regulation. The regulator is robust to variation in the  $k$  parameters, the plant matrices, and the exogenous inputs when an internal model is included as in Eqn. (20).

Regulator design is contingent on properties of the open loop plant as follows:

**Theorem 2.1.** [2] *Necessary and sufficient conditions for structurally stable regulation are*

1.  $(A, B)$  stabilizable
2.  $(C, A)$  detectable
3. Rank  $\begin{bmatrix} \lambda_i - A & B \\ C & 0 \end{bmatrix} = n + p$  for  $\lambda_i$  an eigenvalue of  $Z$

The third condition requires the plant transmission zeros to be different than the spectrum of  $Z$ . Furthermore, there must be at least as many controls as there are outputs. Since it is always possible to reduce the number of controls, we will henceforth assume  $p = m$ , so the system is square.

Theorem 2.1 specifies the open loop system  $\{A, B, C\}$  for which robust regulation is possible. Now consider robust regulation failure. The system matrix for  $\{A(\vartheta), B(\vartheta), C(\vartheta)\}$  is

$$\Gamma_{\vartheta}(s) = \begin{bmatrix} sI - A(\vartheta) & B(\vartheta) \\ C(\vartheta) & 0 \end{bmatrix} \quad (7)$$

A necessary condition for a local exponentially stable equilibrium solution for Eqn. (5) is that

$$\begin{bmatrix} A(\vartheta) & B(\vartheta) \\ C(\vartheta) & 0 \end{bmatrix} \begin{bmatrix} \delta x \\ \delta u \end{bmatrix} = \begin{bmatrix} E \\ F \end{bmatrix} \delta \vartheta \quad (8)$$

obtains an  $[\delta x \ \delta u]^T$  for all  $\delta \vartheta$ . Hence,  $\Gamma_{\vartheta}(0)$  must be full rank.

**Definition 2.4.** *The set of points in parameter space on which regulation fails is the singular surface,*

$$\{\vartheta \in R^k : \det \Gamma_{\vartheta}(0) = 0\}$$

The system matrix  $\Gamma_{\vartheta}(s)$  can lose rank due to a zero at the origin and also due to a defect in the input  $B$  or output  $C$  matrices. The singular surface is dimension  $k - 1$ , or codimension one in the parameter space. Since  $\Gamma_{\vartheta}$  is either a regular or singular pencil for fixed  $\vartheta$ , the singular surface partitions the parameter space into disjoint sets. Theorem 2.2 parallels [8].

**Theorem 2.2.** *Consider a region of the parameter space bisected by the singular surface. A robust regulator designed for one half of the space will be unstable in the adjacent half space for generic systems.*

The singular surface divides the original family of plants into sub-families. A robust regulator designed for a subfamily of system Eqn. (4) will fail to stabilize adjacent sub-families.

*Proof:* Loss of simultaneous regulation at a singular surface is introduced in [3] and proved in [8].

Traversing a singular surface is a sufficient but not a necessary condition for loss of stability. Loss of stability is certain at the singular surface. Loss of stability is possible within an open region of the parameter space. In summary, the singular surface partitions the parameter space. The resulting disjoint regions are a starting point for multiple model controller selection.

### 3 Multiple Model Adaptive Control

The multiple model adaptive regulation design subproblems, controller covering and switch logic, are introduced.

#### 3.1 Covering

Due to Theorem 2.2, a multiple model approach is employed to regulate the parameter dependent family of plants  $\mathcal{P}$  of form Eqn. (4). The set of controllers must encompass the family of plants  $\mathcal{P}$ .

**Definition 3.1.** *Covering Problem: Given a range of plant parameters  $\vartheta$ , design a set of controllers  $\mathcal{C}$  such that each plant  $p(\vartheta) \in \mathcal{P}$  is stabilized by at least one  $C_i \in \mathcal{C}$ .*

A generic multiple model control structure is illustrated in Fig. 1. Here each  $C_i$  regulates some region of  $\mathcal{P}$  and each  $p(\vartheta) \in \mathcal{P}$  is regulated by at least one  $C_i \in \mathcal{C}$ . Previous authors, for example [5, 7], design controllers for a finite set of plant models and then employ robustness metrics to ensure  $\mathcal{P}$  is covered. In this paper, controllers are designed for regions  $\Omega_i$  in the parameter space as defined in Sec. 4.2 and these regions cover  $\mathcal{P}$ , i.e.  $\{p(\vartheta) | \vartheta \in \bigcup \Omega_i\} \supseteq \mathcal{P}$ .

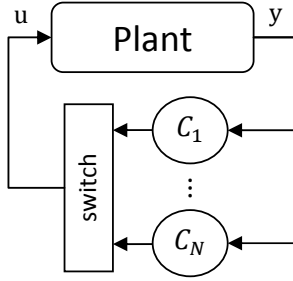


Figure 1. MULTIPLE MODEL CONTROL STRUCTURE

The use of a CQLF for MMAC was proposed in [7]. The convex MMAC method introduced in [10] and summarized in Sec. 4.1 utilizes convexity in plants  $p(\vartheta)$  when possible.

### 3.2 Switching

**Definition 3.2.** Switch Logic Design: *Given a plant family  $\mathcal{P}$  and a control covering  $\mathcal{C}$ , design a switching logic that guarantees convergence to a stabilizing regulator for the “true” plant.*

A CQLF produces a scalar metric that can be tested to ensure stability. A Lyapunov function for the  $i$ 'th convex polytope  $\Omega_i$  with final state  $x_f$ ,

$$V_i = (x - x_f)^T P_i (x - x_f) \quad (9)$$

is monitored for the “in the loop” controller. If the Lyapunov function is decrescent, i.e.

$$V_i(\tau + dt) < V_i(\tau) \quad (10)$$

as shown in Fig. 2, then the correct controller has been identified.

If the “on” Lyapunov function ceases to be decrescent, a different controller is switched on. At least one stabilizing controller exists by design. The controllers are tried “in the loop.” For more detail see the prerouted switch logic in [6]. For the linear quadratic case a Lyapunov function with bounds  $0 \leq V(x) \leq k_2 \|x\|_2$ ,  $\frac{d}{dt}V(x) \leq -k_3 \|x\|_2$  has a time rate of change [12]

$$\dot{V} \leq -\frac{k_3}{k_2}V \quad (11)$$

where  $k_2 = \lambda_{\max}P$  and  $k_3 = \lambda_{\min}C_z^T C_z$  and  $P$  and  $C_z^T C_z$  are symmetric positive definite matrices defined in Sec. 4.1. Combine Eqns. (9), (10), and (11) and  $\tilde{x} = x - x_f$  for the switch logic inequality

$$\tilde{x}(\tau + dt)^T P_i \tilde{x}(\tau + dt) \leq \varphi \tilde{x}(\tau)^T P_i \tilde{x}(\tau)$$

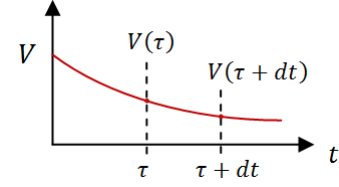


Figure 2. LYAPUNOV FUNCTION  $V$  WITH  $\frac{d}{dt}V < 0$

The switch threshold  $\varphi$  at discrete sampling intervals is

$$e^{-\frac{\lambda_{\min}C_z^T C_z}{\lambda_{\max}P} \cdot dt} \leq \varphi < 1 \quad (12)$$

In general, the unknown final state  $x_f = \lim_{t \rightarrow \infty} x(t)$  is a function of the parametric uncertainty, exogenous disturbances, and controller gains. Although the disturbance estimation form of linear regulation [13] provides an estimate of the exogenous input  $\vartheta$ , and the Lyapunov function Eqn. (11) is convex in  $\vartheta$  per Eqn. (8), estimation of  $x_f(\vartheta)$  is beyond the scope of this note. Since the regulator design of Sec. 4.4 only requires bounds on the parametric uncertainty and is independent of the exogenous disturbances, this paper assumes that the unknown component of  $\vartheta$  is arbitrarily small in relation to Eqn. (11).

## 4 Regulator Design

A Common Quadratic Lyapunov Function (CQLF) is sought for subfamilies of the parameter dependent family of plants  $\mathcal{P}$ . This section adapts the LMI method in [14], pg. 115 to provide state feedback gains and CQLFs for systems of type Eqn. (4).

### 4.1 LQR as LMI

The quadratic LQR problem can be expressed as a Linear Matrix Inequality (LMI). Given a linear system

$$\dot{x} = Ax + Bu, \quad z = C_z x + D_z u \quad (13)$$

with state feedback control  $u = Kx$  the LQR problem of minimizing the energy  $\int_0^\infty z^T z dt$  can be solved by the inequality

$$\begin{bmatrix} AQ + QA^T + BY + Y^T B^T & (C_z Q + D_z Y)^T \\ C_z Q + D_z Y & -I \end{bmatrix} < 0 \quad (14)$$

which is a function of system parameters  $A$  &  $B$ , design weights  $C_z$  &  $D_z$ , and is convex in the symmetric matrix variable  $Q > 0$ . Here  $Y = -(D_z^T D_z)^{-1} B^T$  with Lyapunov matrix  $P = Q^{-1}$ . The

above LMI is equivalent to the quadratic Riccati matrix inequality via the Shur complement

$$A^T P + PA + C_z^T C_z - PB (D_z^T D_z)^{-1} B^T P \leq 0$$

The controller is  $K = YQ^{-1} = - (D_z^T D_z)^{-1} B^T P$ .

## 4.2 Block LMI

The LQR design problem is cast as an LMI in Eqn. (14) for a single plant. In this section the LQR design problem is cast as an LMI for a set of plants. A double index notation will be used for points  $\vartheta_{ij}$  where the index  $i$  signifies the region  $\Omega_i$  and the index  $j$  signifies the point. Composition of regions  $\Omega_i$  is detailed in the following Sec. 4.3. Now extend the inequality (14) to a subfamily of plants.

**Definition 4.1.** *The image of the set of points  $\{\vartheta_{ij}\}$  under  $p(\cdot)$  is the set of plants  $\{p(\vartheta_{ij})\}$ . A set of LMIs for  $\{p(\vartheta_{ij})\}$  is a block LMI.*

In particular, consider the block LMI where the inequality (14) is enforced at each point  $\vartheta_{ij}$  in  $\Omega_i$ ,

$$\begin{bmatrix} LMI(\vartheta_{i1}) & & & \\ & LMI(\vartheta_{i2}) & & \\ & & \ddots & \\ & & & LMI(\vartheta_{in}) \end{bmatrix} < 0 \quad (15)$$

This block LMI is formed by substituting

$$A \rightarrow \bar{A}(\vartheta_{ij}), B \rightarrow \bar{B}(\vartheta_{ij})$$

into Eqn. (14) at points  $\vartheta_{ij} \in \{\vartheta_{i1}, \vartheta_{i2}, \dots, \vartheta_{in}\}$  to obtain a set of inequalities for simultaneous solution. Details of  $\bar{A}(\vartheta_{ij}), \bar{B}(\vartheta_{ij})$  are left to Sec. 4.4. Section 4.3 provides guidance on selecting  $\{\vartheta_{ij}\}$ .

Each block LMI Eqn. (15) obtains a stabilizing controller  $C_i$  with state feedback control  $K_i$  and Lyapunov function matrix  $P_i$  for the continuous set of plants  $\{p(\vartheta) | \vartheta \in \Omega_i\}$ . The state feedback control is

$$K_i = - (D_z^T D_z)^{-1} B_i^T P_i \quad (16)$$

with Lyapunov function matrix  $P_i = Q_i^{-1}$ . Choose a  $B_i$  such that

$$B_i \in Co\{B(\vartheta_{ij})\} \quad (17)$$

to obtain a constant  $K_i$ . It can be shown that if Eqn. (15) holds for all  $B(\vartheta_{ij})$  and  $B_i$  is chosen according to Eqn. (17), then a solution  $P_i$  of the block LMI

$$A_{CL}^T(\vartheta_{ij}) P_i + P_i A_{CL}(\vartheta_{ij}) + Q_i < 0 \quad (18)$$

with  $A_{CL}(\vartheta_{ij}) = A(\vartheta_{ij}) + B(\vartheta_{ij}) K_i$  exists. The  $P_i$  of Eqn. (18) may need to be used in place of the  $P_i$  of Eqn. (15) for the switch logic of Sec. 3.2 if either  $\{B(\vartheta_{ij})\}$  is nonsingleton or if the  $LMI(\vartheta_{ij})$  in Eqn. (15) are assigned different  $C_z, D_z$ , i.e.  $D_z(\vartheta_{ij})$ .

The distinction between LMI and block LMI is convenient for assembling the inequalities. A numerical solver makes no distinction between an LMI and a set of LMIs.

## 4.3 Finite Set of Plants

The previous Sec. 4.2 obtains an CQLF for a finite set of plants, but the set of points  $\{\vartheta_{ij}\}$  used to define region  $\Omega_i$  is not defined. Choosing  $\{\vartheta_{ij}\}$  to represent region  $\Omega_i$  is the goal of this section. Linear and nonlinear systems are considered separately.

If system Eqn. (1) is linear and the map  $\vartheta \rightarrow \Gamma(\vartheta)$  is linear in  $\vartheta$ , then the image of  $\Omega$  under  $\Gamma(\cdot)$  is convex. Thus, plant matrices  $\{A(\vartheta), B(\vartheta), C(\vartheta)\}$  of each  $\{p(\vartheta) | \vartheta \in \Omega_i\}$  can be written as a convex combination of vertices  $\{\vartheta_{ij}\}$  of a polytope  $\Omega_i$  in parameter space. A convex parameter space ensures a convex equilibrium surface where the solution to Eqn. (8) exists. The polytopic region  $\Omega_i$  is defined by the convex hull ( $Co$ ) of its vertices, i.e.

$$\Omega_i \equiv Co\{\vartheta_{ij}\} \quad (19)$$

The block LMI computation uses a small set of polytope vertices  $\{\vartheta_{ij}\}$ . An example is presented in [10].

For the general nonlinear system Eqn. (1) with map  $\vartheta \rightarrow \Gamma(\vartheta)$  continuous in  $\vartheta$ , the plant matrices  $\{A(\vartheta), B(\vartheta), C(\vartheta)\}$  of each  $\{p(\vartheta) | \vartheta \in \Omega_i\}$  may not be convex in  $\vartheta$ . For example, the tangent manifold of a nonlinear system is not a convex function of the state in general, regardless of the parameter dependence. A grid may be applied to the parameter space and local convexity conveys to grid tiles. The grid must be sufficiently dense to capture variation in  $\Gamma(\vartheta)$ . This block LMI computation uses a possibly large set of grid vertices  $\{\vartheta_{ij}\}$ . An example is presented in Sec. 5.3.

When  $\mathcal{P}$  has a diverse zero structure then two or more regions  $\Omega_i$  will be needed. Figure 3 is an example of regions  $\Omega_i$  covering the parameter space of  $\mathcal{P}$ . In the case of linear systems, the regions are convex polytopes (e.g.  $\Omega_1$ ), but for nonlinear systems the regions are in general not convex. Per Theorem 2.2, if for any  $\vartheta \in \Omega_i$ ,  $|\Gamma_\vartheta(0)| = 0$ , then  $\Omega_i$  contains singular surface and neither a common regulator nor a CQLF exist for all  $\vartheta \in \Omega_i$ . The singular surface is a natural partition for plant subfamilies.

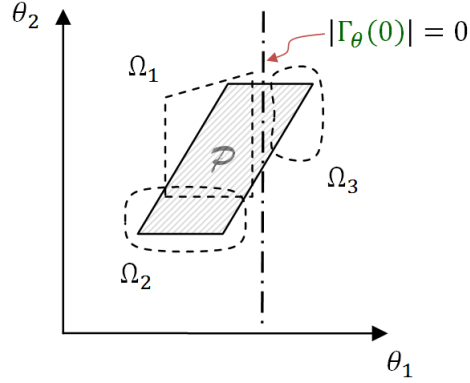


Figure 3. REGIONS COVERING THE PARAMETER SPACE

#### 4.4 Regulator Type

Now apply Eqn. (15) to design the set of controllers  $\{C_1, \dots, C_N\}$  of the multi-model controller in Fig. 1. Two categories of regulator design are described in [13] and only the “Error Augmentation” regulator design method is convex. A “Disturbance Estimation” regulator design is shown to be a Bilinear Matrix Inequality in [10] due to the design degrees of freedom of the observer model. Error augmentation type controllers [13, 15] use an explicit copy of the disturbance model Eqn. (2). This controller is driven by the error dynamics and an observer is not required. The design steps are

1. Define error driven dynamic system that incorporates  $p$  copies of the disturbance model,

$$\dot{\eta} = Z\eta + Je \quad (20)$$

where  $J$  is chosen such that  $(J, Z)$  is controllable.

2. Form the composite system from Eqns. (2) & (4),

$$\begin{bmatrix} \dot{x} \\ \dot{\eta} \end{bmatrix} = \begin{bmatrix} A(\vartheta) & 0 \\ JC(\vartheta) & Z \end{bmatrix} \begin{bmatrix} x \\ \eta \end{bmatrix} + \begin{bmatrix} B(\vartheta) \\ 0 \end{bmatrix} u$$

Solve for the stabilizing state feedback control

$$u = [K_x \ K_\eta] \cdot \begin{bmatrix} x \\ \eta \end{bmatrix} \quad (21)$$

The composite plant matrices for use in Eqn. (15) are

$$\bar{A}(\vartheta_{ij}) = \begin{bmatrix} A(\vartheta_{ij}) & 0 \\ J_i C(\vartheta_{ij}) & Z \end{bmatrix}, \bar{B}(\vartheta_{ij}) = \begin{bmatrix} B(\vartheta_{ij}) \\ 0 \end{bmatrix} \quad (22)$$

## 5 Example

Regulation to the equilibrium surface of a longitudinal aircraft dynamics model with diverse zero structure is considered. Two equilibrium sheets are identified and two controllers sufficient to stabilize the family of plants are obtained.

### 5.1 Longitudinal Aircraft Dynamics

Consider the longitudinal dynamics of a generic aircraft [3]. This system has four states and two outputs ( $n = 4, p = 2$ ). The state vector  $x = [v, \alpha, \theta, q]^T$  is comprised of velocity  $v$ , angle of attack  $\alpha$ , pitch  $\theta$ , and pitch rate  $q$ . The system has two inputs ( $m = 2$ ), thrust  $\Pi$  and elevator  $\delta$ . The a priori unknown parameters are the center of gravity location  $\kappa$ , the commanded velocity  $v^*$ , and the commanded flight path angle  $\gamma^*$  where  $\gamma = \theta - \alpha$ .

The system may be written in the form of Eqn. (1) as

$$\begin{aligned} f(x, u, \vartheta) &= R(v, \alpha)^{-1} \cdot M(x, u, \vartheta) \\ h(x, u, \vartheta) &= \{v - v^*, \gamma - \gamma^*\} \end{aligned} \quad (23)$$

where the flight path angle is  $\gamma = \theta - \alpha$  and  $v^*$  and  $\gamma^*$  are the commanded velocity and flight path angle. The equations of motion  $M(x, u, \vartheta)$  can be found by  $\Sigma F_x$ ,  $\Sigma F_z$ , and  $\Sigma M_y$  about a body fixed axis

$$M(x, u, \vartheta) = \begin{bmatrix} -W \sin \theta - D \cos \alpha + L_w \sin \alpha \\ W \cos \theta - D \sin \alpha - L_w \cos \alpha \\ q \\ c_1 (M_w + \kappa L_w \cos \alpha) - c_2 q \end{bmatrix} + \begin{bmatrix} \Pi + L_t \sin \alpha_t \\ -L_t \cos \alpha_t \\ 0 \\ -c_1 (1 - \kappa) L_t \cos \alpha_t \end{bmatrix}$$

The rotation from body to wind coordinates  $R(v, \alpha)$  is

$$R(v, \alpha) = \begin{bmatrix} \cos \alpha & -v \sin \alpha & v \sin \alpha & 0 \\ \sin \alpha & v \cos \alpha & -v \cos \alpha & 0 \\ 0 & 0 & 1 & 0 \\ 0 & 0 & 0 & 1 \end{bmatrix}$$

The aerodynamic functions are normalized

$$\text{Weight} = W = 1, \quad \text{Drag} = D = \rho v^2 (a + b F_w^2),$$

$$\text{Lift (wing)} = L_w = \rho v^2 F_w, \quad \text{Lift (tail)} = L_t = \rho v^2 F_t$$

where lift is cubic in  $\alpha$  and elevator  $\delta$ ,

$$F_t = \frac{d}{\alpha_0} (\alpha - \alpha_0 + \delta - 3(\alpha - \alpha_0 + \delta)^3)$$

$$F_w = \frac{1}{\alpha_0} (\alpha - 2.08(\alpha - \alpha_0)^3)$$

$$\alpha_t = \alpha + \delta, \alpha_0 = \frac{1}{20}, a = \frac{1}{20}, b = \frac{1}{20}, c_1 = 300, c_2 = 8, d = \frac{1}{10}$$

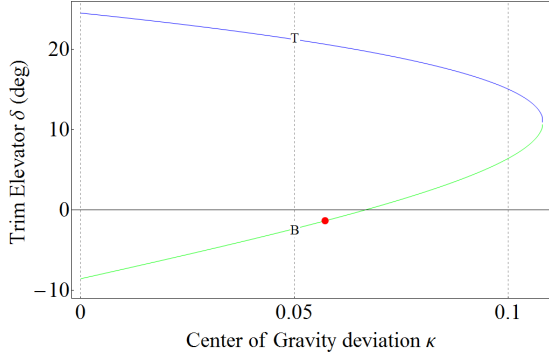


Figure 4. EQUILIBRIUM CURVE  $\delta$  VS.  $\kappa$  AT FIXED VELOCITY

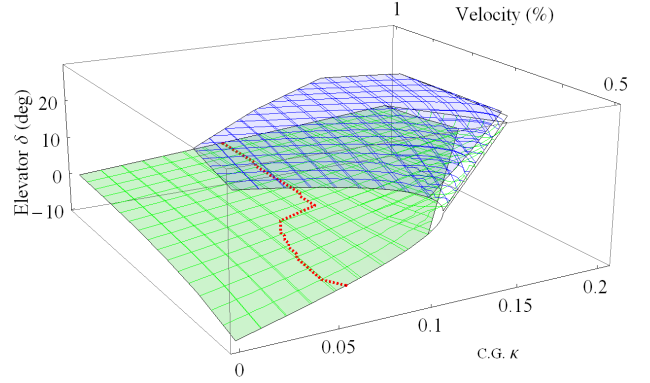


Figure 5. EQUILIBRIUM SHEETS

with  $\rho = 1$  and a wing moment  $M_w$  of zero. Envelope, actuator, and parameter constraints are as follows. Note that only level flight is considered here. Velocity is normalized by maximum cruise velocity.

$$0 \leq v \leq 1, -0.5 \leq \delta \leq 0.5, 0 \leq \Pi \leq 1 \quad (24)$$

$$0.5 \leq v^* \leq 1, \gamma^* = 0, 0 \leq \kappa \leq 0.2 \quad (25)$$

## 5.2 Equilibrium Manifold

A one and two dimensional equilibrium surface is computed for the longitudinal aircraft dynamics.

**5.2.1 One Parameter Curve** When the velocity  $v^*$  and flight path angle  $\gamma^*$  commands are known the equilibrium constraint  $\mathcal{E} = 0$  is  $n + p = 6$  equations with  $n + m + k = 7$  variables and the equilibrium surface is dimension one. Equilibrium values for the elevator angle  $\delta$  as a function of  $\kappa$  at a fixed velocity and level flight trim condition  $(v^*, \gamma^*) = (0.5, 0)$  are shown in Figure 4. Only the portion of the equilibrium curve below the red dot on the bottom branch at  $\kappa \approx 0.057$  is open loop stable.

For the one dimensional equilibrium surface of Fig. 4 the codimension 1 singular surface corresponds to the point (dimension zero) where  $\frac{\partial \dot{q}}{\partial \delta} = 0$ . The  $B$  matrix element at row four, column two changes sign at the singular surface which is the nose of the curve in Fig. 4 where the two branches of the equilibrium surface meet. The two branches meet at approximately  $\kappa = 0.12$  and vanish for  $\kappa > 0.12$ .

**5.2.2 Two Parameter Surface** When only the flight path angle command  $\gamma^*$  is known the equilibrium constraint  $\mathcal{E} = 0$  is  $n + p = 6$  equations with  $n + m + k = 8$  variables and the equilibrium surface has dimension two. The equilibrium equation  $\mathcal{E}(x, u, \vartheta) = 0$  may be solved by noting that  $q = 0$  at steady

state and specifying  $v^*$  such that  $\kappa$  is the independent variable; thus  $\mathcal{E}$  is reduced to three equations in variables  $\alpha, \Pi, \delta$ . Repeat this process over the domain of  $\{v^*, \kappa\}$  in Eqn. (25) to form a set of points  $\mathcal{E}^*$  per Eqn. (3).

The two dimensional equilibrium surface is plotted in Fig. 5 in coordinates  $(\kappa, v, \delta)$  as the unshaded mesh. The shaded portions of the mesh equilibrium surface correspond to control covering as described in Sec. 5.4.1. The portion of the equilibrium sheet below the dashed red line is open loop stable. Whereas the 1-D equilibrium curve has branches, the disjoint sets of the 2-D equilibrium surface will be called sheets. In this example, the top and bottom sheets of the equilibrium surface may be distinguished by the sign of  $\det \Gamma$  in Eqn. (7). The surface area of the top equilibrium sheet of Fig. 5 is smaller than the bottom equilibrium sheet due to enforcement of constraints Eqn. (24).

The independent variables used to compute the equilibrium surface are the parameters  $(v^*, \kappa)$ . Observe that the equilibrium surface of Fig. 5 is multi-valued in coordinate  $\kappa$  due to the top and bottom sheets. Two parameterizations are

1. An atlas with two charts: For this example the coordinates  $(v^*, \kappa, \sigma^*)$  where  $\sigma^* \in \{B, T\}$  are sufficient. Here  $B, T$  enumerate the Bottom and Top equilibrium sheets respectively. The coordinate set  $(v^*, \alpha^*, \sigma^*)$  is similar but employs a measurable state. The use of measurable coordinates combined with fore knowledge of the equilibrium surface may facilitate final state  $(x_f)$  computation.
2. Local parameterization: The equilibrium surface may be locally parameterized as a composition of flows of the span of the null space as suggested in [16]. In this case, the equilibrium surface is parameterized by coordinates  $s_1, s_2$ . For example, choose as an origin the singular surface point along the velocity slice  $v = 0.6$  to obtain  $\delta(s_1, s_2) \approx 0.25 + s_1$ ,  $\alpha(s_1, s_2) \approx 0.12 + s_2$ . This injective parameterization may be superior for control design near the singular surface.

**Remark 5.1.** In the case of multiple equilibrium sheets, two or

more sheets may have similar zero structure such that regions on these disjoint sheets share common quadratic stability. A parameterization different from the above may be desired. This parameterization arranges the tangent bundle subspace  $\Gamma_{\vartheta}$  according to common quadratic stability. The mapping from parameter space  $\vartheta$  to the elements of  $\{A(\vartheta), B(\vartheta), C(\vartheta)\}$  of Eqn. (4) would be onto but not one-to-one. For this shared stability case a simple equivalence test for common quadratic stability would be helpful but such a test is an open problem.

### 5.3 Family of Plants

The process of Sec. 2.1 is used to obtain a linear family of plants from the equilibrium surface of the nonlinear dynamics. The equilibrium constraint  $\mathcal{E} = 0$  for system Eqn. (23) is  $n + p = 6$  equations in  $n + m + k = 9$  variables with  $k = 3$  parameters:  $(v^*, \gamma^*, \kappa)$ . This example considers only level flight ( $\gamma^* = 0$ ) such that  $k = 2$  and the equilibrium surface is 2-D as shown in Sec. 5.2.2 and Fig. 5.

Evaluate the linearization equations along the equilibrium surface  $\mathcal{E}^*$  to obtain a finite set of approximately 150 plants for regulator design. This finite set is a subset of the continuous family  $\mathcal{P}$  as represented by the shaded regions of the equilibrium surface in Fig. 5. The finite subset excludes  $p(\vartheta) \in \mathcal{P}$  near the singular surface where for this example controllability is lost.

As an example of the family  $\mathcal{P}$  consider plants taken from the two equilibrium branches of Fig. 4. The plants are taken from the bottom and top equilibrium branches as shown by “B” and “T” along the line  $\kappa = 0.05$  in Fig. 4 (where  $v^* = 0.5$ ). The linearized plant from the bottom branch shown in Row 1 of Table 1 is located inside the region of open loop stability. The linearized plant from the top branch shown in Row 2 of Table 1 has a zero structure different from the bottom branch sub-family of plants and is open loop unstable.

TABLE 1. LINEARIZED PLANT ( $\kappa = 0.05$ )

Surface	A	B
Bottom	$\begin{bmatrix} -0.73 & -0.67 & -1 & 0 \\ -7.7 & -10.1 & 0 & 1 \\ 0 & 0 & 0 & 1 \\ 0 & -64.3 & 0 & -8 \end{bmatrix}$	$\begin{bmatrix} 0.98 & 0.03 \\ -0.38 & -0.92 \\ 0 & 0 \\ 0 & -126.5 \end{bmatrix}$
Top	$\begin{bmatrix} -0.64 & -0.89 & -1 & 0 \\ -7.8 & -7.9 & 0 & 1 \\ 0 & 0 & 0 & 1 \\ 0 & 232.7 & 0 & -8 \end{bmatrix}$	$\begin{bmatrix} 0.98 & -0.19 \\ -0.38 & 1.3 \\ 0 & 0 \\ 0 & 170.5 \end{bmatrix}$

### 5.4 Regulator Design

The following two sections obtain the  $\{P_i\}$  for switch logic and the  $\{K_i\}$  for control covering.

**5.4.1 Common Quadratic Lyapunov Function** A CQLF matrix  $P_i$  which satisfies Eqn. (18) is obtained by simul-

taneously solving sets of inequalities (14) in the block LMI of Eqn. (15) as detailed in Sec. 4. The composite design matrices of Sec. 4.4 are

$$A_j = \begin{bmatrix} A(\vartheta) & 0 \\ JC & Z \end{bmatrix}, B_j = \begin{bmatrix} B(\vartheta) \\ 0 \end{bmatrix}$$

and are uniquely defined by coordinates  $\vartheta = (v^*, \kappa, \sigma)$ . The parameter dependent matrices  $A(\vartheta)$  and  $B(\vartheta)$  were obtained in the preceding section. For this example matrices  $C$  and  $F$  are independent of  $\vartheta$  and thus identical for all  $p(\vartheta) \in \mathcal{P}$ . The regulated outputs are  $[v \ \gamma]^T = Cx$ , the set-points  $v^*, \gamma^*$  are mapped to the outputs with a binary matrix  $F$  as follows,

$$C = \begin{bmatrix} 1 & 0 & 0 & 0 \\ 0 & -1 & 1 & 0 \end{bmatrix}, F = - \begin{bmatrix} 1 & 0 \\ 0 & 1 \end{bmatrix}$$

The state disturbance  $E$  may translate the equilibrium as needed.

The regulator design matrices for the internal model  $Z$  and error update gains  $J$  are  $J = I_2, Z = 0_2$ .

The composite plant plus controller state vector  $\bar{x}$  is dimension  $n + p = 6$ ,

$$\bar{x} = [v, \alpha, \theta, q, \eta_1, \eta_2]^T$$

The LQR design weights of (13) have form

$$[C_z \ D_z] = \begin{bmatrix} Q_z & 0 \\ 0 & R_z \end{bmatrix}$$

where for both subfamilies  $Q_z = I_{n+p}, R_z = I_p$ .

The composite design matrices  $A_j, B_j$  and design weights  $C_z, D_z$  are used in Eqn. (14) to form approximately 100 and 50 inequalities for the bottom and top surface respectively. These inequalities are concatenated into LMIs of form Eqn. (15) and solved for a CQLF. A single CQLF was obtained for each of the top and bottom equilibrium surface regions seen as shaded portions of Fig. 5. Since controllability is lost at the singular surface the unshaded portions of Fig. 5 are not guaranteed stable by the CQLFs. Given the above design weights the CQLF for the top equilibrium sheet is

$$P_T = \begin{bmatrix} 3.9 & -1.6 & -0.16 & -0.06 & 0.96 & 0.5 \\ -1.6 & 4.8 & 0.29 & 0.29 & -0.12 & -0.02 \\ -0.16 & 0.29 & 2.4 & 0.08 & -0.91 & 1.2 \\ -0.06 & 0.29 & 0.08 & 0.04 & -0.03 & 0.03 \\ 0.96 & -0.12 & -0.91 & -0.03 & 5.5 & -0.22 \\ 0.5 & -0.02 & 1.2 & 0.03 & -0.22 & 2.1 \end{bmatrix}$$

**5.4.2 State Feedback Controller** Recall that a single matrix  $B_i \in Co\{B(\vartheta_{ij})\}$  is used to form the LQR state feedback gain  $K_i = -(D_z^T D_z)^{-1} B_i^T P_i$  for the region  $\Omega_i$ . In general choose  $B_i$  such that  $\|K\|_2$  is minimized to improve robustness to unmodeled error. In this example the matrix  $B(\vartheta_{ij})$  that minimizes  $\|B(\vartheta)\|_2$  over  $\vartheta \in \Omega_i$  was chosen as  $B_i$ . This selection



of  $B_i$  for Eqn. (16) per Eqn. (17) such that Eqn. (18) holds is detailed in Table 2.

TABLE 2. SELECTION OF  $B_i$  TO MINIMIZE  $\|K\|_2$

Sheet	Region	$\vartheta$ coordinates( $v^*, \kappa, \sigma^*$ )	$\ K\ _2$
Bottom	$\Omega_B$	$\vartheta_{ij} = (0.5, 0.1, B)$	3.20
Top	$\Omega_T$	$\vartheta_{ij} = (0.6, 0.15, T)$	10.97

The state feedback of Eqn. (21) is

$$K_B = \begin{bmatrix} -2.2 & 0.24 & 0.16 & 0.01 & -0.91 & -0.77 \\ -0.4 & 0.79 & 2.4 & 1. & -0.73 & 1.3 \end{bmatrix}$$

$$K_T = \begin{bmatrix} -4.1 & 2.5 & 0.22 & 0.12 & -0.98 & -0.5 \\ 1.8 & -9.8 & -2.5 & -1.2 & 0.96 & -1.2 \end{bmatrix}$$

The previous Sec. 5.4.1 solves inequalities Eqn. (14) simultaneously in the block form of Eqn. (15) for a  $P_i$ . However, if upon selection of  $B_i$ , Eqns. (18) do not hold with this  $P_i$ , then with inputs  $B_i$  and  $K_i$  simultaneously solve inequalities Eqns. (18) in block form to alter  $P_i$  for use in switch logic Eqn. (9). For the choices of  $B_i$ ,  $i \in \{B, T\}$ , in Table 2, only  $P_B$  must be altered by solving Eqns. (18).

## 5.5 Simulation

In case of an unanticipated change in the aircraft longitudinal dynamics, the “true” longitudinal dynamics may be imprecisely known. As shown in Sec. 2.2, a single regulator may fail to simultaneously regulate the aircraft due to zero structure change. The two locations on the equilibrium curve listed in Table 1 and pictured in Fig. 4 are simulated. The aircraft is nominally trimmed to the open loop stable “Bottom” plant when an event occurs at  $t = 1$  sec. The “true” plant for  $t \geq 1$  is then the “Top” plant. The zero structure and coordinate  $\sigma$  changes. Just two state feedback controllers are sufficient to regulate all plants in  $\mathcal{P}$ .

Details of the plant and controller simulation components can be found in the following subsections:

1. Plant Family  $\mathcal{P}$ : Section 5.3, Table 1.
2. Control Gains  $K_i$ : Section 5.4.2
3. Switch Logic: Section 3.2
4. CQLF  $P_i$ : Section 5.4.1

These four components are assembled into the MMAC structure of Fig. 1. The MMAC is simulated in Mathematica. Initial conditions for the plant ( $x$ ), controller ( $\eta$ ), exogenous disturbance ( $\vartheta$ ), switch logic index ( $\sigma$ ) states and parameters ( $v^*, \kappa, \sigma$ ) are specified as follows

$$\begin{aligned} [v(0) \ \alpha(0) \ \theta(0) \ q(0)] &= [1.1v^* \ \alpha^* \ 1.1\theta^* \ q^*] \\ [\eta_1(0) \ \eta_2(0)] &= [0 \ 0] \\ [\vartheta_1(0) \ \vartheta_2(0)] &= [v^* \ 0] \\ \sigma(0) &= B \\ (v^*, \kappa) &= (0.5, 0.05) \\ \sigma^* &= \begin{cases} B & t < 1 \\ T & t \geq 1 \end{cases} \end{aligned}$$

The simulation timeline is shown in Table 3.

TABLE 3. SIMULATION TIMELINE

Time	Plant Eq. Sheet ( $v^*, \kappa, \sigma^*$ )	Lyapunov Metric ( $\dot{V}_i$ )	Switch Logic State ( $\sigma(t)$ )
$t < 1$	(0.5, 0.05, B)	$\dot{V}_B < 0$	$\sigma \rightarrow B$
$t = 1$	plant dynamics change		
$t > 1$	(0.5, 0.05, T)	$\dot{V}_T < 0$	$\sigma \rightarrow T$

The final value of the composite state is defined as

$$\bar{x}^*(v^*, \kappa, \sigma^*) \equiv [v^* \ \alpha^* \ \theta^* \ q^* \ \eta_1^* \ \eta_2^*]$$

where  $q^* = 0$  and  $\theta^* - \alpha^* = \gamma^*$ . The controller states ( $\eta_1^*, \eta_2^*$ ) are zero if the parameter values are equilibrium values. In other words, if ( $v^*, \gamma^*, \kappa$ ) are consistent with an equilibrium point  $\mathcal{E}(x^*, u^*, \vartheta^*) = 0$ , then  $\eta_i^* = 0$ . For  $t \geq 1$  the final state is

$$\bar{x}^*(0.5, 0.05, T) = [0.5 \ 0.116 \ 0.116 \ 0 \ 0 \ 0]$$

The bounded Lyapunov functions  $V_i$ ,  $i \in \{B, T\}$ , of Fig. 8 show internal stability. The Lyapunov functions are normalized such that  $V(0) = 100\%$ . The time rate of change of the Lyapunov functions  $V_i$ ,  $i \in \{B, T\}$  are shown in Fig. 7. The switch logic quickly responds ( $< \frac{1}{100}$  secs) as seen in Fig. 6(a). Thus  $K_B$  regulates toward an equilibrium on the “Bottom” sheet for  $t < 1$  and then the correct controller,  $K_T$  is quickly switched on for  $t > 1$ . Successful output regulation  $\lim_{t \rightarrow \infty} e(t) = 0$  is shown in Fig. 6(b).

## 6 Conclusions

A multiple model adaptive regulator is implemented for a parameter dependent, longitudinal aircraft dynamics model with zero structure change. A finite set of controllers is obtained for plant subfamilies with equivalent zero structure. For this dynamics model, two controllers are sufficient for regulation in a neighborhood of the equilibrium surface over a large portion of

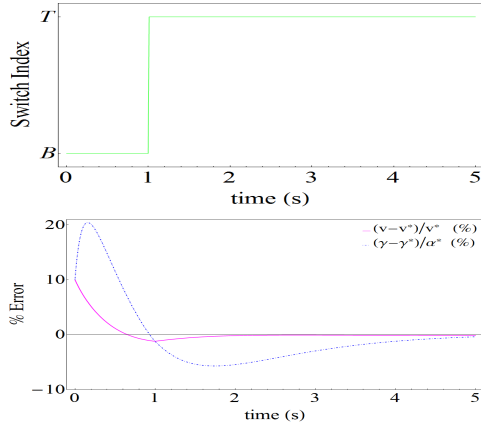


Figure 6. (a) SWITCH INDEX  $\sigma$  (ABOVE); (b) REGULATION ERROR  $e$

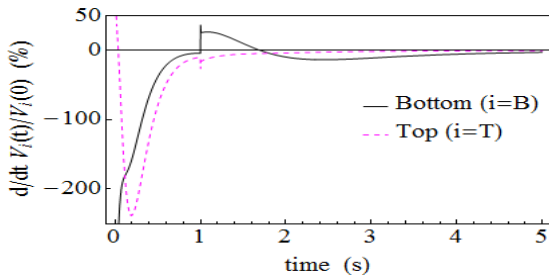


Figure 7. NORMALIZED LYAPUNOV RATE:  $\frac{d}{dt} V_i(t)/V_i(0)$  (%)

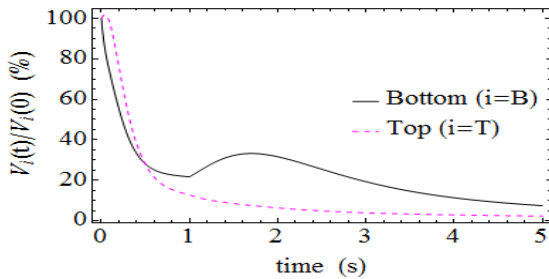


Figure 8. NORMALIZED LYAPUNOV FUNCTION:  $V_i(t)/V_i(0)$  (%)

the flight envelope. Switch logic based on Lyapunov functions ensures that the appropriate stabilizing controller is chosen. The multi-model design subproblems are solved concurrently as a set of linear matrix inequalities. The design is suitable for complex systems since fast, accurate solutions of large LMIs are possible.

In summary, it is well known that regulation is not possible at points of zero structure change. Less well known is that regulation by a common controller is not possible across points of zero structure change. Thus, a common controller can only be used as parameters vary within a family having equivalent zero structure. The finite set of controllers with switch logic enables robust adaptive regulation.

## REFERENCES

- [1] Kwakernaak, H., and Sivan, R., 1972. *Linear optimal control systems*. Wiley-Interscience New York.
- [2] Francis, B. A., 1977. "The linear multivariable regulator problem". *SIAM Journal on Control and Optimization*, **15**, pp. 486–505.
- [3] Kwatny, H. G., Bennett, W. H., and Berg, J. M., 1991. "Regulation of relaxed stability aircraft". *IEEE Transactions on Automatic Control*, **AC-36**(11), pp. 1325–1323.
- [4] Narendra, K. S., and Annaswamy, A. M., 1989. *Stable adaptive systems*. Prentice Hall.
- [5] Anderson, B. D. O., 2000. "Multiple model adaptive control. part 1: Finite controller coverings". *International Journal of Robust and Nonlinear Control*, **10**, pp. 909–929.
- [6] Angeli, D., and Mosca, E., 2002. "Lyapunov-based switching supervisory control of nonlinear uncertain systems". *IEEE Trans. on Automatic Control*, **47**(3), pp. 500–505.
- [7] Boskovic, J. D., 2008. "An integrated approach to damage accommodation in flight control". In AIAA Guidance, Navigation, & Control Conference.
- [8] Berg, J., and Kwatny, H. G., 1994. "An upper bound on the structurally stable regulation of a parameterized family of nonlinear control systems". *Systems and Control Letters*, **23**, pp. 85–95.
- [9] Morse, A. S., 1997. "Supervisory control of families of linear set-point controllers - part 2. robustness". *Automatic Control, IEEE Transactions on*, **42**(11), pp. 1500–1515.
- [10] Peterson, E., and Kwatny, H., 2014. "Multi-model adaptive regulation for a family of systems containing different zero structures". In IFAC World Congress, Vol. 19, p. To Appear.
- [11] Francis, B. A., and Wonham, W. M., 1975. "The internal model principle for linear multivariable regulators". *Applied mathematics and optimization*, **2**(2), pp. 170–194.
- [12] Khalil, H., 2002. *Nonlinear Systems*. Prentice Hall, New Jersey.
- [13] Kwatny, H. G., and Kalnitsky, K. C., 1978. "On alternative methodologies for the design of robust linear multivariable regulators". *IEEE Transactions on Automatic Control*, **AC-23**(5), pp. 930–933.
- [14] Boyd, S., El Ghaoui, L., Feron, E., and Balakrishnan, V., 1994. *Linear Matrix Inequalities in System and Control Theory*. SIAM, Philadelphia, PA.
- [15] Davison, E. J., 1972. "The output control of linear time-invariant multivariable systems with unmeasurable arbitrary disturbances". *IEEE Transactions on Automatic Control*, **AC-17**(5), pp. 621–630.
- [16] Kwatny, H. G., and Chang, B. C., 1998. "Constructing linear families from parameter-dependent nonlinear dynamics". *IEEE Transactions on Automatic Control*, **43**(8), pp. 1143–1147.